Journal of Medicinal and Chemical Sciences 6 (2023) 677-692

Journal of Medicinal and Chemical Sciences

Journal homepage: http://www.jmchemsci.com/

Original Article

Synthesis and Characterization of Bulky and Nano Complexes of Telmisartan with Some Heavy Metal Ions (Ru^{3+} and Au^{3+}) and Their Anticancer Activity

Zahraa Q. Mahdi[1], Mahasin F. Alias[1]*

Department of Chemistry, College of Science for Women, University of Baghdad, Iraq

ARTICLE INFO

Article history

Receive: 2022-06-06
Received in revised: 2022-08-16
Accepted: 2022-10-03
Manuscript ID: JMCS-2209-1699
Checked for Plagiarism: **Yes**
Language Editor:
Dr. Fatimah Ramezani
Editor who approved publication:
Dr. Mehrdad Hamidi

DOI:10.26655/JMCHEMSCI.2023.3.24

KEYWORDS

Antitumor Agents
Heavy Metal
Nanoscale
Telmisartan
Ultrasonication

ABSTRACT

New complexes of Telmisartan (Telm.) were prepared in this research, where telmisartan used as a chelating agent with trivalent heavy metal ions of ruthenium and gold. The complexes were prepared by conventional method in bulky size, and characterized in solid state by using different measurements included: the spectroscopic analysis acts by UV-Vis and FT-IR, metal composition percent and other elements (C, H, and N) analysis, physical measurements (color, melting points, magnetic susceptibility, and electrical conductivity). The results obtained from these measurements show the coordination sites for the ligand with the metal ions as bi-dentate through two oxygen atoms of telmisartan and the complexation process was succeeded through the reaction of (2 ligand:1 metal ion). Analytical and spectroscopy studies disclosed octahedral structure for Ru(III) complex and square planner structure of Au(III) complex, also show the electrical nature of Au(III) complex, while the opposite for Ru(III) complex. The bulk complexes were converted into nano scale by using an ultrasonic probe device with a period of about 1.5 hours with rolling every 20 minutes, and then identified by (AFM, XRD, and FTIR) analysis. All prepared complexes were applied as antitumor against MDA-MB-231 cell line *in vitro* by the MTT method by using different six concentrations (12.5, 25, 50, 100, 200, and 400 µ/mL) for 24 hours. In general, the results showed that all complexes have the greatest inhibition rate at a high concentration, but specifically the overall order of inhibition for all compounds is Nano Au-Telm > Nano Ru-Telm > Au-Telm > Ru-Telm > Telm.

GRAPHICAL ABSTRACT

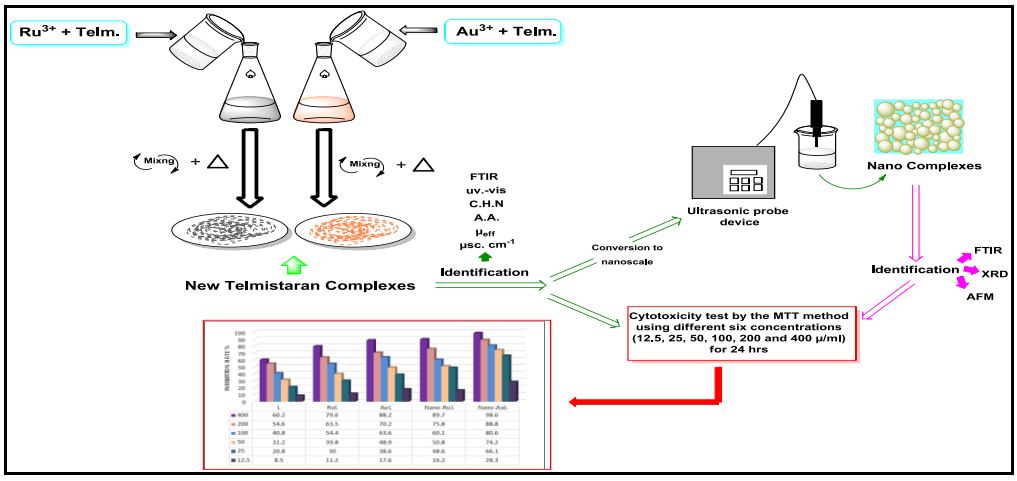

* Corresponding author: Mahasin F. Alias
✉ E-mail: Email: mahasinfa_chem@csw.uobaghdad.edu.iq

Introduction

Telmisartan is an effective angiotensin II receptor antagonist used to treat hypertension, cardiac conditions, heart attacks, and bladder conditions. Telmisartan is now offered as an antihypertensive drug 2 on the market under the trade name MICARDIS [1]. In addition, the beneficial effects against vascular and renal damage brought on by diabetes and cardiovascular disease have been demonstrated for telmisartan. It has been hypothesized that it could also stop the cognitive deterioration in those with Alzheimer's [2].

According to Ries *et al.,* the first total synthesis of telmisartan begins with the acylation of 4-amino-3-methylbenzoic acid methyl ester with butyryl chloride, followed by nitration, reduction of the nitro group, and cyclization of the resultant amine to the benzimidazole derivative. Following saponification, the free carboxyl group is condensed with N-methyl-1,2-phenylenediamine to produce the bis-benzimidazole, which is then alkylated with the 4′-(bromomethyl)-2-biphenylcarboxylic acid tert-butyl ester to produce Telmisartan, with eight steps being the most extended sequence, in 21% overall yield [3, 4].

Transition-metal complexes are appealing targets for the development of catalysts and useful materials [5], as when the metal ions, especially transition metals attach to the organic ligands exhibit different characteristics [6] and due to their distinct electrical and stereo-chemical characteristics, metal complexes have found the extensive usage in the chemical and physical sciences. Metal complexes have been suggested and proven to have medical uses for decades [7, 8]. New biologically active substances are created as antitumor agents every year, some of these substances are chemicals as organic compounds [9] and others as inorganic complexes [10] or metal-organic frameworks [11]. Likewise, numerous studies have looked into the possibility of employing specific medications as chelating agents to create metal complexes that are biologically active [12].

Previous investigations were successful in creating metal complexes of telmisartan with other metallic elements, including telmisartan Organo-tin (IV) frameworks, and uses as capture media of CO_2 in the research of Angham G. Hadi *et al.* [13], also Zn(II) complexation and mechanisms of action enhance telmisartan's anticancer activities in the studies of Valeria R. Martínez *et al.* [14, 15]. Another study by María S. Islas *et al.* [16] involved the preparation of the octanuclear complex of copper(II)-telmisartan and showed its biological effects. In addition, the study of Shaista Bano *et al.* [17] where included the complexation of telmisartan with Y(III) and Nd(III), etc. The current work is concerned with the use of telmisartan as a ligand to form complexes with ruthenium and gold ions and tested as an anticancer.

Materials and Methods

Solvents and the chemicals that used in the process of synthesis of new compounds were supplied from Sigma-Aldrich and Merck. Stuart Melting Point Apparatus was used to measure melting points of the result complexes. The UV-Visible spectrophotometer UV-1601 was employed to determine the absorbance wavelength by using a quartz cuvette and ethanol as the reference. The Fourier Transform Infrared (FT-IR) spectra were recorded for free ligands and metal complexes in the 4000-200 cm^{-1} on an FT-IR 8300 Shimadzu Spectrophotometer. Elemental microanalysis C.H.N have been accomplished on the metal complexes were nominated through the micro-analytical unit at Euro EA3000 elemental analyzer. Atomic absorption was conducted by using (Atomic Absorption Spectrophotometry AA-6880 Shimadzu). The molar conductivities were measured for the complexes at 10^{-3} M in solution of ethanol complexes at R.T by using ProfiLine Oxi 3205 Instrument. The magnetic susceptibility measurements were obtained at R.T by using (MSB–MKI) magnetic susceptibility moder balance. The XRD analysis measured for the complexes in the laboratory of Kashan University in Iran by using X-ray Diffract meter Shimadzu 6000 instrument. To prepare the nanoparticles of complexes used the ultrasonic probe model intelligent ultrasonic processor UCD-150. The AFM measurements were recorded in Al-Nahrain University, Collage of science laboratory by the

instrument Veeco's Atomic Force Microscope Instruments Inc. of Plainview, NY, USA. The antitumor tests were carried out in the laboratory of the College of Science, Al-Nahrain University.

General procedure to prepare complexes from Telmisartan (Telm.)

Solution of telmisartan (2 mmole, 0.102 g) in 96% ethanol at pH =7 (adjusted by the addition of aqueous solution 1M of NaOH), was stirred at 70 °C. Then, a solution of $RuCl_3.H_2O$ (0.207 g, 1 mmol) and $HAuCl_4$ (0.205 g, 1 mmol) in 5 mL of ethanol was left at ambient temperature, and upon 24 hours evaporation and obtained a color powder. The color solid was filtered, washed with mixture of hot ethanol and water to remove as NaCl, and air-dried; the analytical and physical properties are summarized in Table 1.

Preparation of nanomaterial of heavy metals-Telm complexes by using ultrasonic probe

The nanomaterial was prepared by using the Top-Down method [18] via an ultrasonic probe device with a period of about 1.5 hours with rolling every 20 min.

0.125 g of these heavy complexes Ru-Telm and Au-Telm were taken and placed in 250 mL beakers, and then 50 mL of distilled water added to them because dis. water does not dissolve these complexes. After that the beakers were placed in the ultrasonic probe machine for 1.5 hours with cooling intervals in an ice bath every 20 minutes. After beating the solution for 1.5 hours, 1 mL of the solution was taken for the AFM measurement. The result was left to evaporate the water and the precipitate was taken for the other measurements like (XRD, FT-IR, etc.).

Preparation of the bulk and nano-complexes used in cytotoxicity assay

Four stock solution of work complexes Ru-Telm and Au-Telm (bulk and nano size) were prepared. Each stock was made by dissolving 0.0004 g (400 µg/mL) of the work complexes, and then diluted in DMSO to obtain (12.5, 25, 50, 100, and 200) µg/mL as well as to control and used for cytotoxicity assay on MDA.MB.231 cell line.

Results and Discussion

A. Bulky structure

The ligand used in this work (Telm.) is white and the metal complexes are colored with their good percentage yields ranging from 78% and 86.21%, as presented in Table 1. Both prepared compounds are steady toward light and air and soluble in ethanol. The metal complexes were characterization by several analytical methods like (C.H.N elemental analysis, A.A metal analysis, UV-Vis; FT-IR, magnetic moment measurements, and the molar conductivities). It was noted that the results of the analytical and experimental data are in agreement. The result proves that complexes ionic nature of the gold complex and the value of the magnetic susceptibility of prepared complexes is assent with the proposed molecular geometry of them. Physio-chemical characters of ligand and its metal complexes are listed in Table 1.

FT-IR spectra of telmisartan and its metal complexes

The main characteristic experimental vibration of telmisartan, Ru(III), and Au(III) complexes obtained from infrared are depicted in Table 2 and Figures 1, 2 and 3.

The strong band at 1695 cm^{-1} is associated with C=O stretching of carboxylic acid in free ligand [19] and a weak a broad band which appeared at 3403 cm^{-1} and other at 1288 cm^{-1} which corresponding to –OH stretching mode and C-OH carboxylic group [20], other bands can be observed in Table 2.

$$Inhibition\ rate\% = \frac{Absorbtion\ of\ negative\ control - Absorbtion\ of\ test}{Absorbtion\ of\ negative\ control} \times 100$$

Table 1: The physiochemical information of telmisartan ligands and two prepared metal complexes

Compound	Color	Molecular weight g/mol	Melting point (°C)	Yield (%)	Molar ratio M:L	Elemental analysis Cal. (Found)				Suggested formula
						C%	H%	N%	M%	
Telm.	White	514.6	263.26	-	-	-	-	-	-	$C_{33}H_{30}N_4O_2$
Ru-Telm	Black	1199.35	250-248	78.00	1:2	66.07 (65.75)	5.21 (5.67)	9.34 (9.71)	8.42 (8.89)	$C_{66}H_{62}N_8O_6RuCl$
Au-Telm	Orang	1276.40	180-178	86.21	1:2	62.04 (61.75)	4.73 (4.99)	8.77 (8.29)	15.42 (15.11)	$C_{66}H_{64}N_8O_6AuCl$

The carbonyl group of carboxylic acid in complexes was disappeared and new bands was observed in the position 1575 and 1580 cm^{-1} and 1395 and 1390 cm^{-1}, respectively which assigned to both asymmetric and symmetric stretching mode of the carboxylate groups generated by coordination of this group with metal ions. The difference between asymmetric and symmetric frequencies indicated the activity of this ligand as a bidentate through two atoms of oxygen [21].

The complexes spectra exhibited the new weak bands at frequency 542 and 453 cm^{-1}, respectively which assigned to the stretching frequencies of M-O bond [22]. Furthermore, abroad bands were around 3353-3560 cm^{-1} and 3420 cm^{-1}, respectively, belonging to the presence of water molecules out of sphere, and another bands appeared at 902 and 864 cm^{-1} is due to the rocking and wagging bending of water molecules within field of coordination in Ru(III) complex [23].

Table 2: The selected FT-IR bands in cm^{-1} observed in the spectra of ligand and its metal complexes

Compounds	νOH	νCH aliphatic + aromatic	$\nu COO^-_{asym.}$	$\nu COO^-_{sym.}$	Δν	νM-O	Others
Telm.	3403	3305.7 3036 2987 2962	-	-	-	-	νCO =1695 ν CN = 1128 δCH = 740
Ru-Telm	3353 3560	3056 2996 2882	1575	1395	180	542	νCN= 1128 δCH = 740 Ru-Cl = 342 ρOH= 902, 864
Au-Telm	3420	3059 2922 2862	1580	1390	190	453	νCN= 1128 δCH = 740

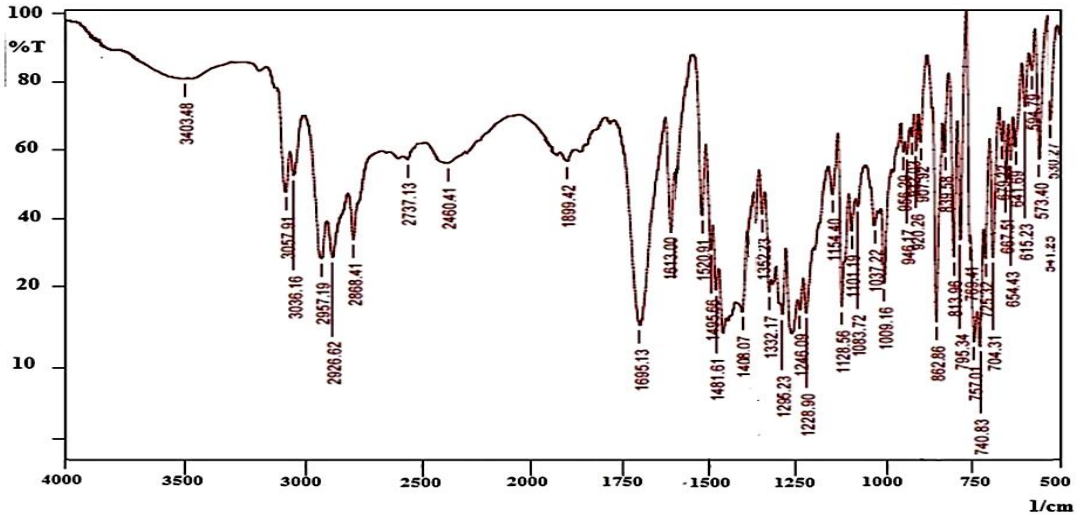

Figure 1: FT-IR spectrum of telmisartan

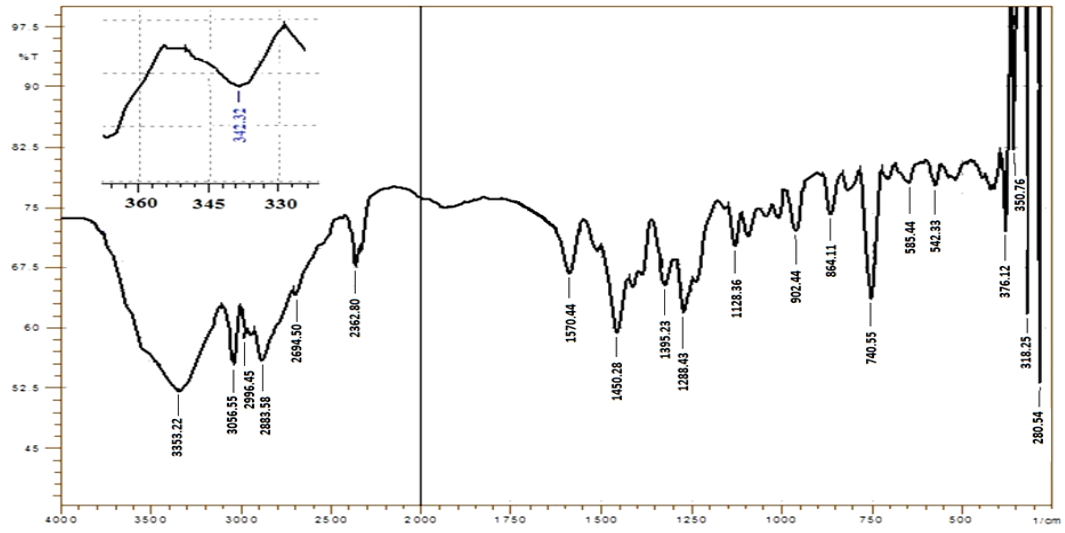

Figure 2: FT-IR spectrum of Ru-Telm

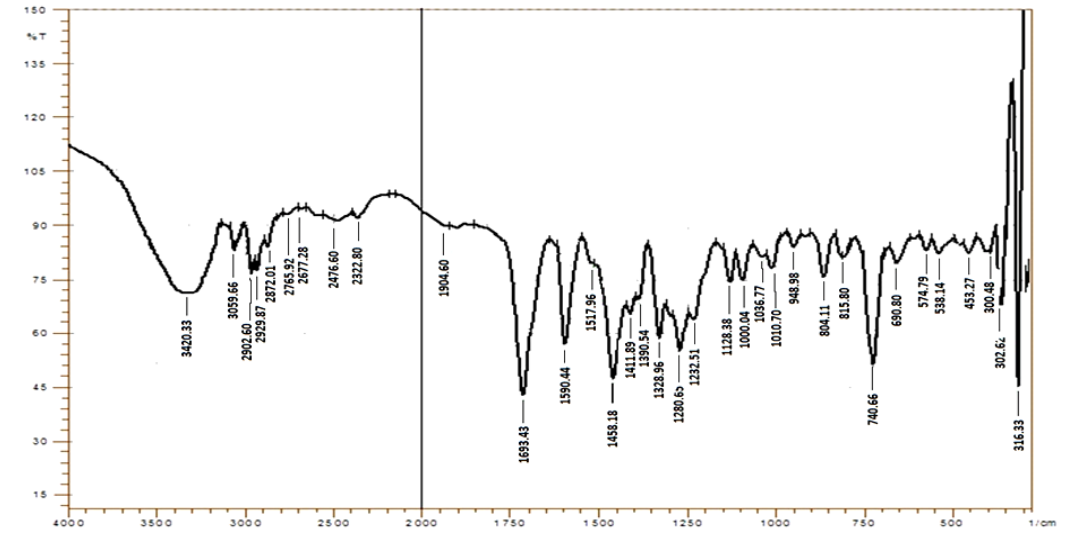

Figure 3: FT-IR spectrum of Au-Telm

The electronic spectrum of telmisartan and its metal complexes

The electronic spectrum of telmisartan (Telm.)

According to the solubility characteristics of the telmisartan drug in ethanol was selected as solvent for analysis, and from scanning of this drug by UV-spectra, the wavelengths were selected for estimation of Telm. at 207 nm (48309 cm^{-1}), 228 nm (43859 cm^{-1}), and 298 nm (33557 cm^{-1}), as demonstrated as in Figure 4.

The first absorption bound which due to inter-ligand transition (π-π*) located on the pi system and the second one arises from (π-π*) transition, but with another group, the third absorption band is attributed to (n-π*) electronic transition location on the nitrogen atoms imidazole ring [24]. These bands submit a shift in the prepared complexes due to the metal-ligand interaction which obviously indicated the coordination of this drug with metal ion, as reported in Table 3.

The electronic spectrum of Ru-Telm. complex

The UV–Vis spectrum of black Ru(III) complex, Figure 5, shows bands at 12738 and 25641 cm^{-1} which are assigned to $^2T_2g \rightarrow {}^4T_1g$ and $^2T_2g \rightarrow {}^2A_2g + {}^2T_1g$ transition, respectively, with $t_2g^5eg^0$ configuration. The values of the 10Dq, Racah parameter, and the missing ν_2 and nephelauxetic factor β were estimated by using Tanab-sugano diagram for octahedral d^5 configuration by fitting the ratio of ν_3/ν_1, which equal to 2.01 fits the diagram at 3.5 Dq/B', the B' was estimated and will be 381 cm^{-1}. The value for constant field splitting 10 Dq was equal to 1330 cm^{-1} at 1330 cm^{-1}. The missing ν_2 band was calculated 18273 cm^{-1} which was assigned to $^2T_2g \rightarrow {}^4T_1g$. This complex is nonelectrolyte and the magnetic moment value (1.85 B.M) is observed and compared with other reporters [25], and this degree with the Oh geometry around Ru(III) ion supposed, as illustrated in Figure 6 and Table 3.

The electronic spectrum of Au-Telm. complex

The spectrum of gold ion was diagnosed by charge transfer bands which dominate the ligand field transitions. This means that these absorption bands results are in an overlap between them which make the interpretation of the spectra more difficult.

The electronic spectrum of this orange complex, Figure 7, showed three main bands at 24570, 28809 as a shoulder, and 31746 cm^{-1} which refers to $^1A_1g \rightarrow {}^1B_1g$, $^1A_1g \rightarrow {}^1Eg$, respectively and the other peak attributed to the charge transfer [26]. The magnetic moment is diamagnetic and the conductivity measurements for this complex are showed to be ionic nature at 45.5 $\mu s.cm^{-1}$.

According to these data, in addition to the data obtained from FT-IR, A.A, and CHN analysis, a square planar can be postulated, as indicated in Figure 7 and Table 3.

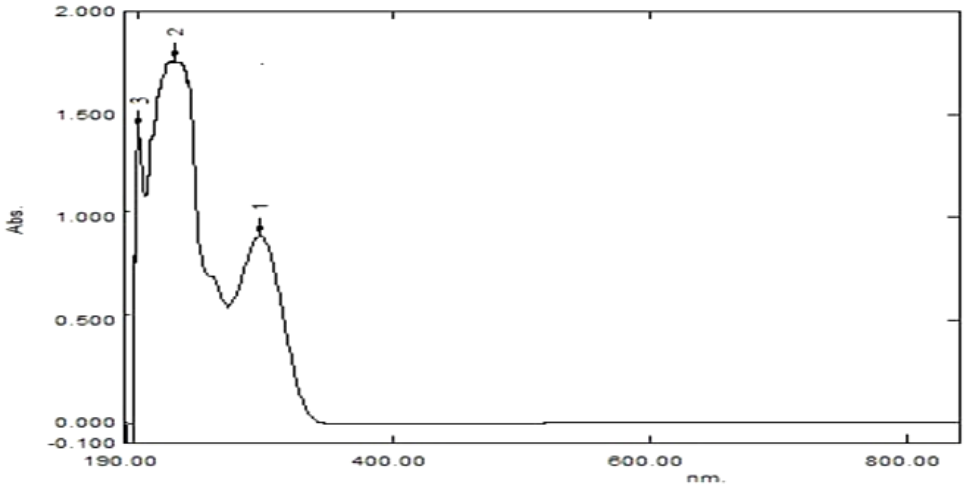

Figure 4: UV-Vis spectrum of telmisartan

Table 3: Probable assignment of electronic spectra of telmisartan and its metal complexes, conductivity measurements, magnetic moments, and proposed geometry of synthesis complexes

Compounds	Abs. cm^{-1}	Assignments	μ_{eff} B.M	conductivity µs. cm^{-1}	Suggested geometry
Telm.	33557 43859 48309	$n \rightarrow \pi^*$ $\pi \rightarrow \pi^*$ $\pi \rightarrow \pi^*$	-	-	-
Ru-Telm	12738 (18273) cal. 25641 33333	$^2T_2g \rightarrow {}^4T_1g$ $^2T_2g \rightarrow {}^4T_2g$ $^2T_2g \rightarrow {}^2A_2g$ + ^2T_1g L→RuCT	1.85	24.4	Octahedral
Au-Telm	24570 28809 31746	$^1A_1g \rightarrow {}^1B_1g$ $^1A_1g \rightarrow {}^1Eg$ L→AuCT	0.00	45.5	Square planar

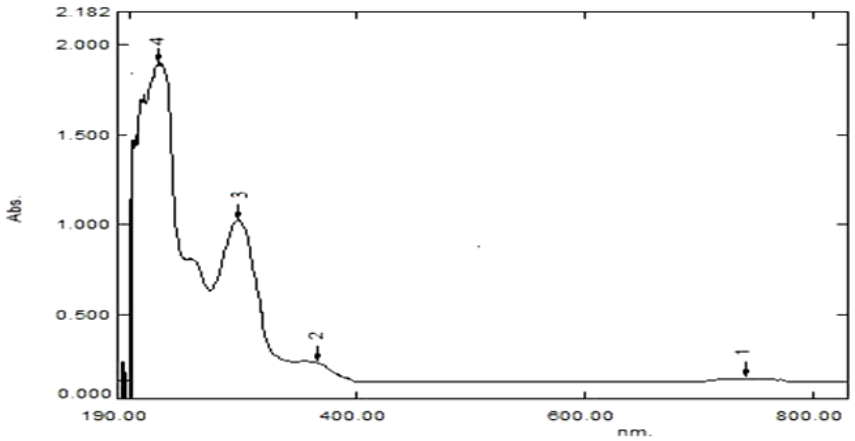

Figure 5: UV-Vis spectrum of Ru-Telm

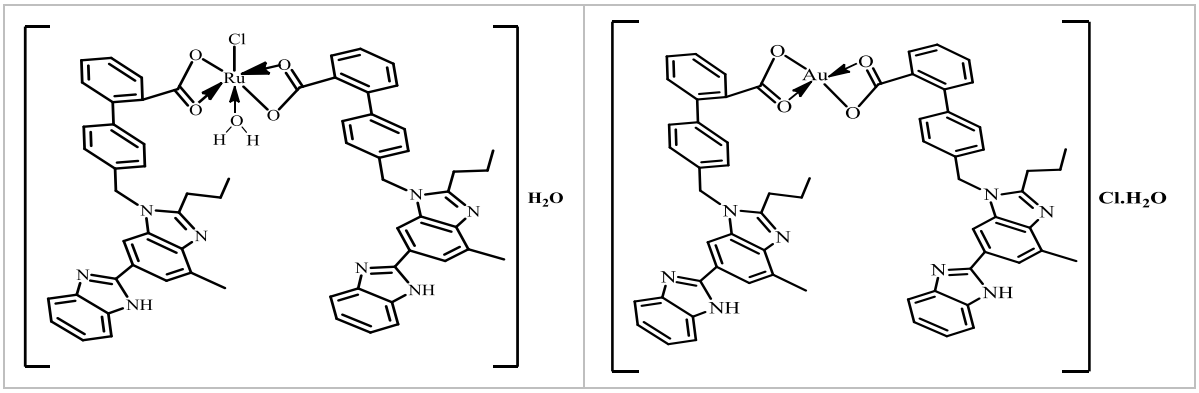

Figure 6: The proposed structures of new prepared complexes

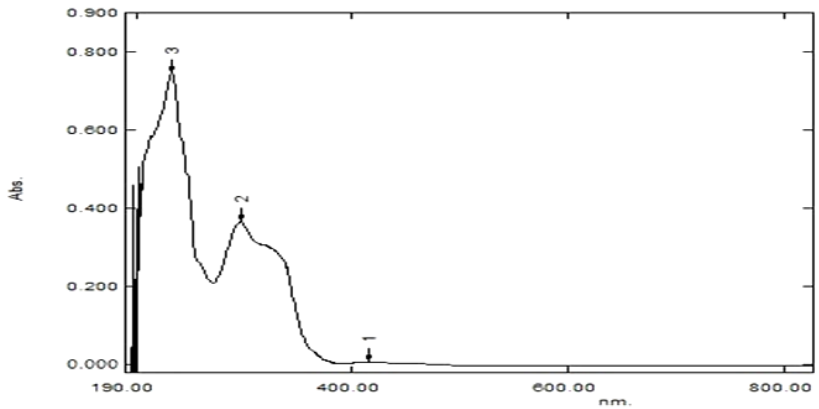

Figure 7: UV-Vis spectrum of Au-Telm

B. Nano structure

The nano complexes of Ru-Telm and Au-Telm were prepared by cracking method, which is one of the physical methods.

Ultrasonic tools were applied in many homogenous and heterogeneous reactions as an agitator or homogenizer. The ultrasound application in chemical reactions provides the specific activation based on an acoustic cavitation phenomenon [27]. Cavitation is defined as the formation, growth, and implosive collapse of bubbles in a liquid.

The nano complexes of each Ru-Telm and Au-Telm, which have been studied for their efficacy against breast cancer, were prepared to compare them with the bulky complexes. There were prepared in the manner of ultrasonic probe. The determination of nano-complexes was done by using AFM, XRD, and FT-IR way.

Atomic force microscopy (AFM)

AFM used to determine the particle size and surface organization of the synthesized materials. Figures 8 and 9 show AFM images for both complexes in three- and two-dimensional view in addition to the histogram and table of granularity accumulation distribution chart.

The results show that the particles diameter is in the range 10-110 nm for Ru-Telm and 10-255 nm for Au-Telm, as shown in Figures 8 and 9.

The shape and geometry of the complexes may have an effect on the period of complexes crushing. It was found that the Oh Ru-complex needs about 20 minutes to obtain the highest percentage of nano complex, but the square planar Au- complex give its higher percentage of nano within 10 minutes.

X-ray diffraction (XRD)

The X-ray diffraction patterns in the 2θ range of (10-80) for synthesized complexes are shown in Figures 10 and 11. In Figure 10 of the Ru-Telm nanoparticles indicated the peak with 2θ at (15.72, 30.48, 36.82, 40.21, 55.75, and 65.33) that matches with founds in the literatures [28], while in Figure 11, the Au-Telm nanoparticles indicated peak with 2θ at (10.38, 15.69, 20.65, and 27.91) that matches with founds in the literatures [29]. In X-ray patterns indicated the prepared complexes had a reflection polycrystalline appearance accurately known irregular crystal isolation. The crystallite size was determined by using Debye Scherer's equation:

$$D = \frac{0.9\lambda}{\beta \cos\cos\theta}$$

Where, D = Crystallite size, λ = the wavelength of the x-ray radiation, λ = 0.15406 nm, θ = the diffraction angle, and β = (FWHM), the full width at half maximum. The result obtained for crystallite size of Ru-Telm and Au-Telm is listed in Table 4.

FT-IR spectra of nano complexes

The FT-IR spectra of nano complexes are demonstrated in Figures 12 and 13, which showed abroad band appear at 3421-3427 cm^{-1} are attributed to the hydroxyl group of water molecule in nano complexes, the other bands appeared at 1575 and 1580 cm^{-1} due to the symmetric stretching and 1395 and 1390 cm^{-1} corresponding to the asymmetric stretching mode of the carboxylate groups binding to metal in complexes. Likewise, at 542 and 453 cm^{-1} refers to the νM-O bond, while νM-Cl appears in Ru-complex at 342 cm^{-1}. This indicates that the complexes do not happen to dissociated but only converts the large particles into small one.

Anticancer activity

The foremost target of most research groups is to find a convenient anticancer drug that can be used efficiently for the treatment of human tumor [30].

Sample: Sample Name	**Code:**Sample Code
Line No.:lineno	**Grain No.:**8667
Instrument:SPM	**Date:**2022-08-25

Avg. Diameter:31.84 nm	**<=10% Diameter:16.00 nm**
<=50% Diameter:28.00 nm	**<=90% Diameter:50.00 nm**

Diameter(nm) <	Volume(%)	Cumulation(%)	Diameter(nm) <	Volume(%)	Cumulation(%)	Diameter(nm) <	Volume(%)	Cumulation(%)
10.00	2.42	2.42	42.00	4.20	78.57	74.00	0.20	99.27
12.00	2.23	4.65	44.00	3.31	81.89	76.00	0.16	99.43
14.00	2.12	6.77	46.00	2.68	84.56	78.00	0.10	99.54
16.00	2.47	9.24	48.00	2.40	86.96	80.00	0.10	99.64
18.00	6.03	15.28	50.00	2.75	89.71	82.00	0.06	99.70
20.00	6.73	22.00	52.00	1.66	91.37	84.00	0.06	99.76
22.00	6.30	28.30	54.00	1.48	92.85	86.00	0.07	99.83
24.00	5.50	33.81	56.00	1.30	94.15	88.00	0.03	99.86
26.00	4.74	38.55	58.00	1.15	95.30	92.00	0.03	99.90
28.00	4.88	43.43	60.00	1.04	96.34	94.00	0.01	99.91
30.00	7.17	50.59	62.00	0.73	97.07	96.00	0.05	99.95
32.00	5.64	56.24	64.00	0.73	97.80	100.00	0.01	99.97
34.00	4.94	61.17	66.00	0.44	98.23	102.00	0.01	99.98
36.00	4.28	65.46	68.00	0.31	98.55	106.00	0.01	99.99
38.00	5.61	71.06	70.00	0.27	98.81	110.00	0.01	100.00
40.00	3.31	74.37	72.00	0.27	99.08			

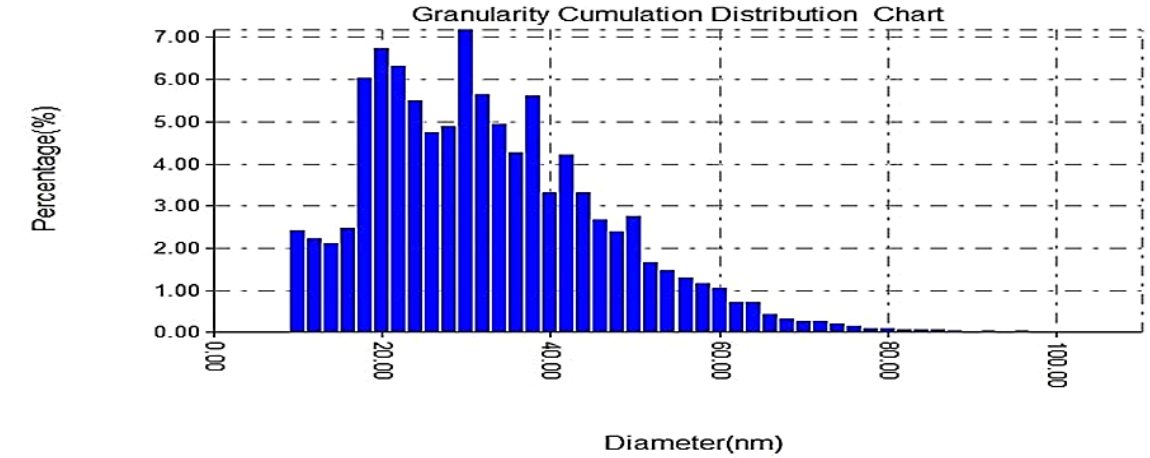

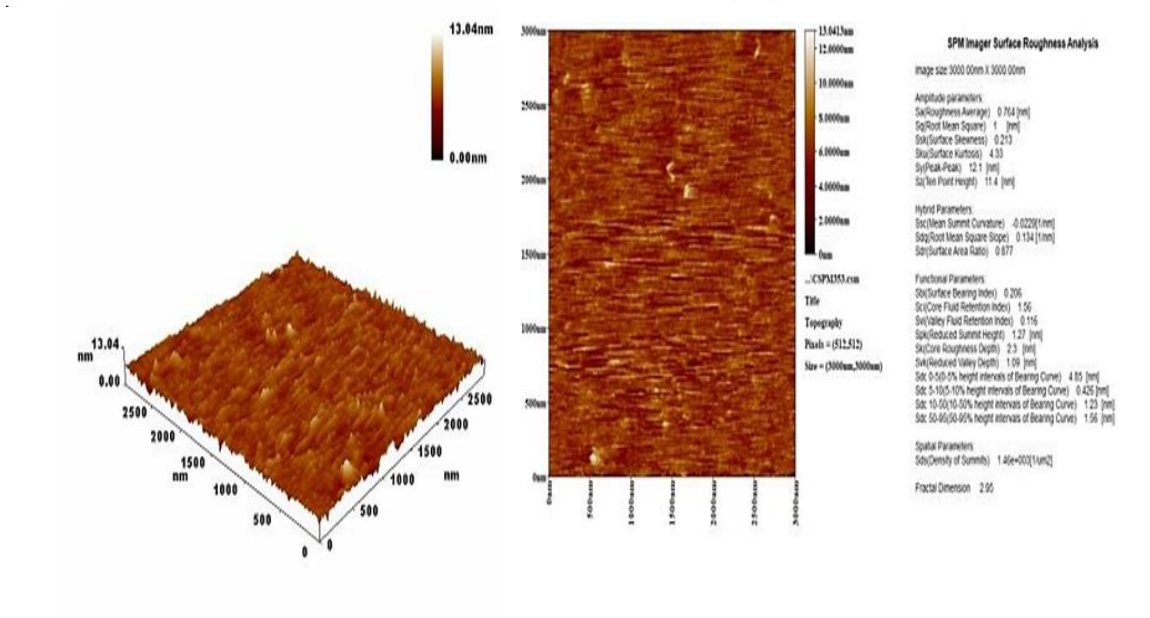

Figure 8: Histograms, table of granularity accumulation distribution, and 2D and 3D view image of Ru-Telm

Sample: Sample Name	**Code:**Sample Code
Line No.:lineno	**Grain No.:**3612
Instrument:SPM	**Date:**2022-08-25

Avg. Diameter:48.91 nm	**<=10% Diameter:20.00 nm**
<=50% Diameter:40.00 nm	**<=90% Diameter:75.00 nm**

Diameter(nm) <	Volume(%)	Cumulation(%)	Diameter(nm) <	Volume(%)	Cumulation(%)	Diameter(nm) <	Volume(%)	Cumulation(%)
10.00	0.08	0.08	75.00	2.96	87.74	140.00	0.17	99.47
15.00	2.44	2.52	80.00	2.96	90.70	145.00	0.11	99.58
20.00	4.79	7.31	85.00	2.24	92.94	150.00	0.08	99.67
25.00	5.92	13.23	90.00	1.33	94.27	155.00	0.06	99.72
30.00	7.39	20.63	95.00	0.83	95.10	160.00	0.03	99.75
35.00	10.35	30.98	100.00	1.41	96.51	165.00	0.03	99.78
40.00	9.16	40.14	105.00	0.69	97.20	170.00	0.06	99.83
45.00	10.47	50.61	110.00	0.78	97.98	175.00	0.06	99.89
50.00	8.39	59.00	115.00	0.44	98.42	180.00	0.03	99.92
55.00	8.42	67.41	120.00	0.36	98.78	195.00	0.03	99.94
60.00	6.56	73.98	125.00	0.22	99.00	200.00	0.03	99.97
65.00	5.84	79.82	130.00	0.17	99.17	255.00	0.03	100.00
70.00	4.96	84.77	135.00	0.14	99.31			

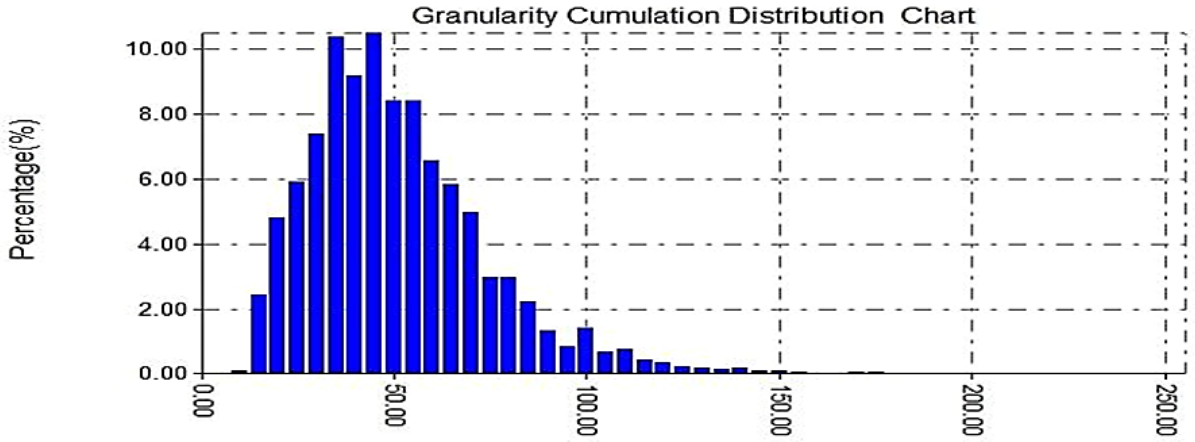

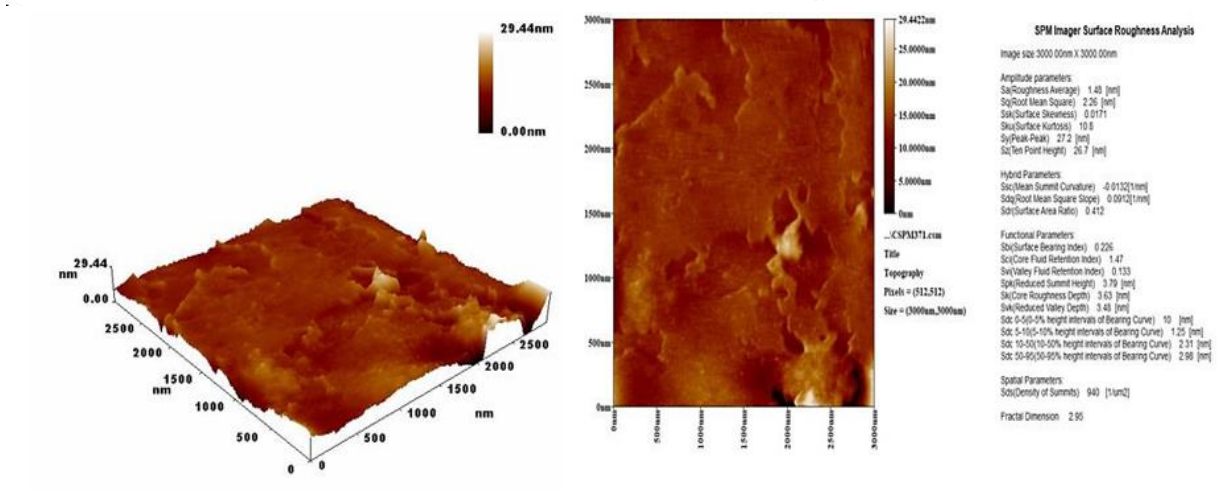

Figure 9: Histograms, table of granularity accumulation distribution, and 2D and 3D view image of Au-Telm

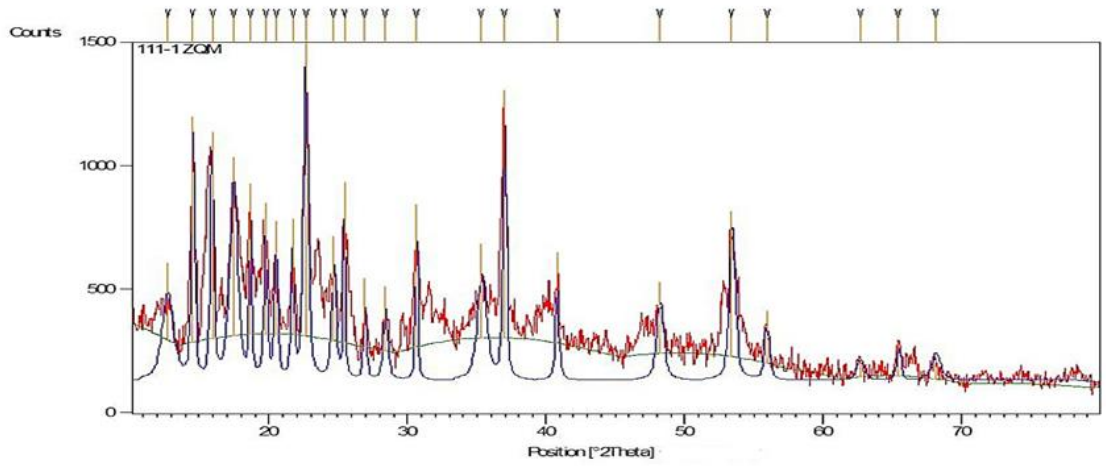

Figure 10: XRD for nanoRu-Telm

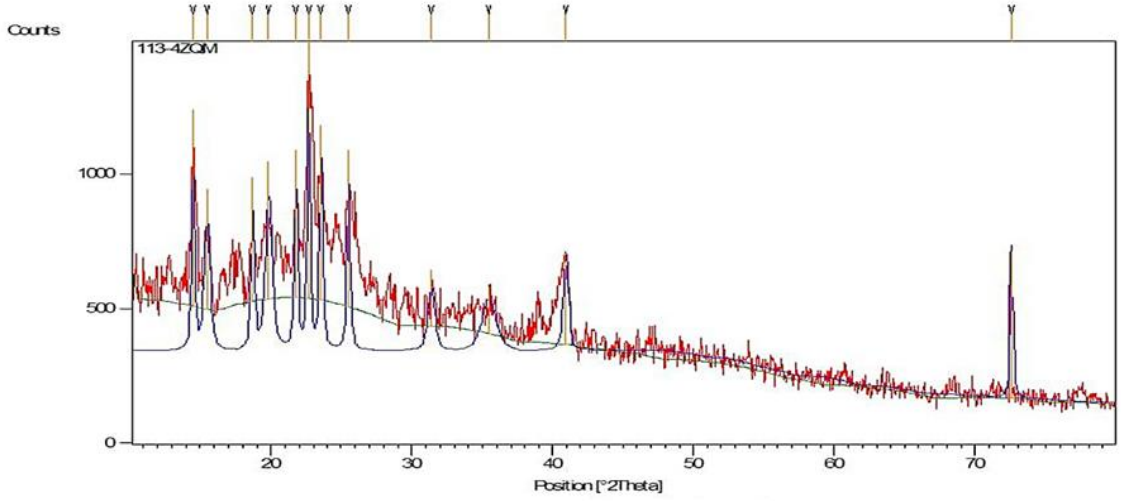

Figure 11: XRD for nanoAu-Telm

Table 4: The calculated crystalline size of the Ru-Telm and Au-Telm with the x-ray result

Compounds	2θ	d (A°)	FWHM (deg.)	intensity (counts)	D(nm)
Ru-Telm	22.65	3.92	0.393	100%	20.68
Au-Telm	22.66	3.91	0.246	100%	33.80

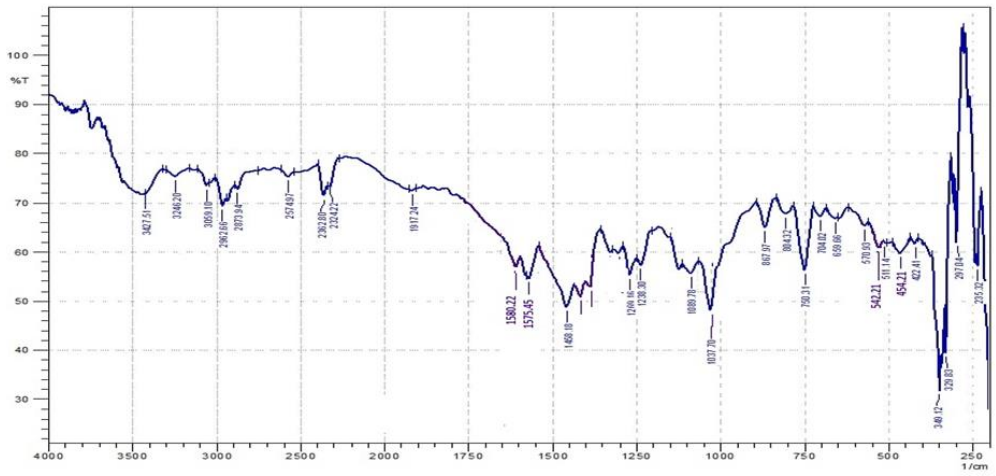

Figure 12: FT-IR for nano Ru-Telm

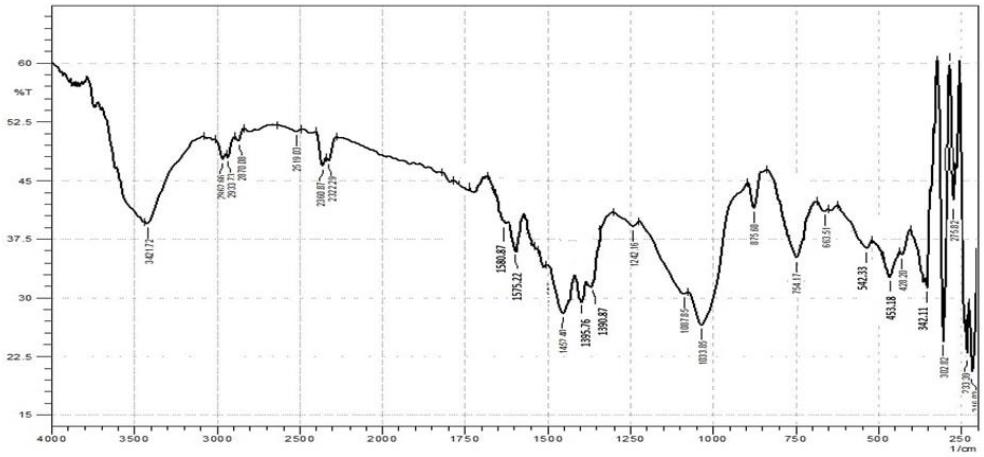

Figure 13: FT-IR for nano Au-Telm

In this work, after 24 h incubation with the new compounds, the cytotoxicity was tested by the MTT method by using different six concentrations (12.5, 25, 50, 100, 200, and 400 µ/ml) for 24 hours and only the cell remain without treatment used as control negative for comparison. Telmisartan and their complexes inhibited the proliferation of MDA-MB-231 cell line *in vitro*, as illustrated in Figure 14 and Table 5. The MMT assay results show the significant grater inhibition rates and better anti-proliferative effect for all complexes as a bulky or nano compounds compared with free ligand. All complexes are significant at all concentrate especially at high concentration. Metal complexes can interfere in cellular redox chemistry in several ways: directly through metal, ligand redox centers, or indirectly by binding to biomolecules involved in cellular redox pathways [14]. The inhibition rates began to reduce gradually from high to low concentration in significant difference ($P<0.01$) at all concentration.

The prior studies have shown that telmisartan inhibits cell proliferation by inducing apoptosis in various types of cancer, including gynecological and urological cancer cell lines. Furthermore, it has been demonstrated that telmisartan induces cell cycle progression, but not apoptosis in esophageal adenocarcinoma [31]. The results of cytotoxic assay of the ligands and their heavy metal complexes on cell line were studied showed that the gold complexes are more toxic than the ligand. This is may be due to geometry of gold complex which has square planner, and the modified surface of gold-NPs grants these agents as a specific function of nanobio admixture which makes molecules able to be used in biomedicine for ideal drug delivery. Gold-NPs are well-known nanoparticles for their significant capability of blending due to their large surface area, which allows them to be conjugated to different chemicals substances, such as various biomolecules. Hence, biosynthesized Au-NPs can be functionalized or adsorbed by biological peptides to deliver drug to a targeted cell/tissue [32]. In addition, for Ru(III) complex a lot of Ru(III) compounds contain exchangeable ligands and require activation by the tumor microenvironment. The antitumor characteristics of the Ru(III) complexes occur when they are reduced to their corresponding Ru(II) counterparts in vivo. Under the biological circumstances of low oxygen concentration, acidic pH and high levels of glutathione, the Ru(II/III) redox potential can be altered, and thus Ru(III) complexes can be readily reduced to Ru(II)-complexes and make more active inside the cell and the subsistence of chloride in the structure of Ru(III) is easily to loss and convert into Ru(II) [33].

From the obtained results, many parameters probably accountable of the leverage of these complexes in pharmacological field like the size of metal, charge allocation, geometry shape, ionic character, polarity, oxidation state of metal, design of substitution of organic compounds “ligands”, and the suggested modes of action of these compounds are either an inhibition of

metalloenzyme DNA-gyrase or an interaction with the DNA molecule via a metal complex intermediate.

Table 5: Statistical data and inhibition rate of ligand and its bulky and nano metal complexes against MDA-MB-231 cell line after 24 hours in lab (*in vitro*)

Inhibition µ/ mL							LSD value
Compounds	400	200	100	50	25	12.5	
Telm	60.2 D a	54.6 D a	40.8 C b	31.2 C c	20.8 E d	8.5 C e	9.42 **
Ru-Telm	79.6 C a	63.5 C b	54.4 B c	39.8 C d	30.0 D e	11.2 BC f	9.05 **
Au-Telm	88.2 BC a	70.2 BC b	63.6 B b	48.9 B c	38.6 C d	17.6 B e	8.95 **
Nano-Ru- Telm	89.7 B a	75.8 B b	60.1 B c	50.8 B d	48.6 B d	16.2 B e	9.06 **
Nano-Au- Telm	98.6 A a	88.8 A b	80.6 A bc	74.2 A cd	66.1 A d	28.3 A e	9.47 **
LSD value	9.07 **	8.60 **	9.67 **	9.01 **	7.92 **	7.13 **	-

Means with different big letters in the same column and small letters in the same row are significantly different.
** (P≤0.01)

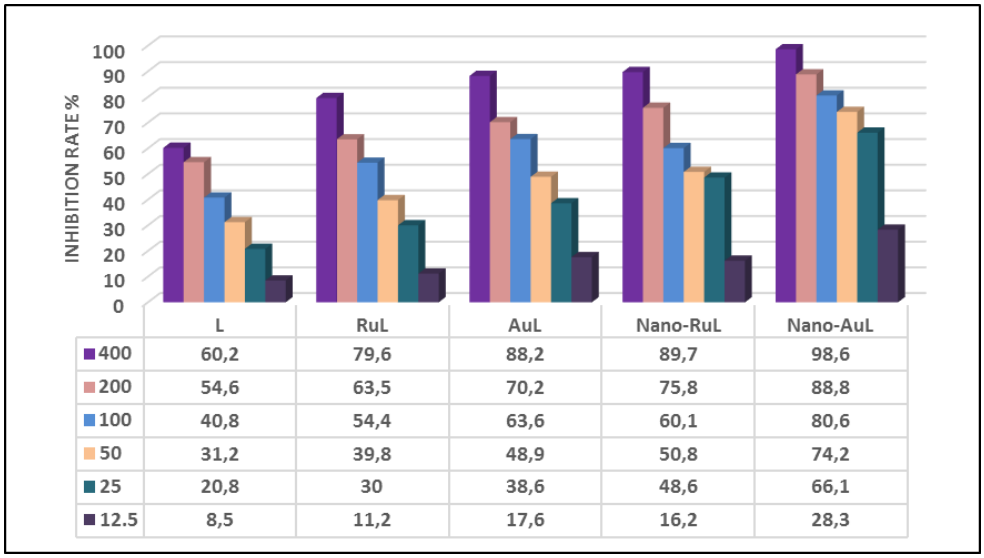

Figure 14: The percentage inhibition in 12.5, 25, 50, 100, 200, and 400 µ/mL after exposure to ligand and its bulky and nano metal complexes at 24 hours

Conclusion

Two novel metal chelates of telmisartan drug in the bulky and nano size were isolated. By using numerous spectroscopic and analytical methods, the structures of these complexes have been demonstrated. The recorded data reveals that the complexes have a 1:2 ratio (metal: ligand) stoichiometry and ligand behave as bidentate through two oxygen atoms. All complexes have a good toxic effect for MDA-MB-231 cells when the results showed *in vitro* growth inhibition of cell line at high concentration (400 µ/mL), while the gold nano complex behave as a better anti-proliferative in all applied concentrations.

Funding

This research did not receive any specific grant from funding agencies in the public, commercial, or not-for-profit sectors.

Authors' contributions

All authors contributed to data analysis, drafting, and revising of the paper and agreed to be responsible for all the aspects of this work.

Conflict of Interest

We have no conflicts of interest to disclose.

ORCID

Mahasin F. Alias
https://orcid.org/0000-0002-3375-1797

References

[1]. Dézsi C.A., The different therapeutic choices with ARBs. Which one to give? When? Why?. *American Journal of Cardiovascular Drugs*, 2016, **16**:255 [Crossref], [Google Scholar], [Publisher]

[2]. Martin A.D., Siamaki A.R., Belecki K., Gupton B.F., A flow-based synthesis of telmisartan, *Journal of Flow Chemistry*, 2015, **5**:145 [Crossref], [Google Scholar], [Publisher]

[3]. Vardanyan R., Hruby V., Synthesis of best-seller drugs. Academic press; 2016 Jan 7 [Publisher]

[4]. Zhang J., Li R., Zhu F., Sun C., Shen J., An improved synthesis of telmisartan via the copper-catalyzed cyclization of o-haloarylamidines, *RSC advances*, 2020, **10**:13717 [Crossref], [Google Scholar], [Publisher]

[5]. Nandy A., Duan C., Taylor M.G., Liu F., Steeves A.H., Kulik H.J., Computational discovery of transition-metal complexes: from high-throughput screening to machine learning, *Chemical Reviews*, 2021, **121**:9927 [Crossref], [Google Scholar], [Publisher].

[6]. Frei A., Metal complexes, an untapped source of antibiotic potential?, *Antibiotics*, 2020, **9**:90 [Crossref], [Google Scholar], [Publisher]

[7]. Karges J., Stokes R.W., Cohen S.M., Metal complexes for therapeutic applications, *Trends in Chemistry*, 2021, **3**:523 [Crossref], [Google Scholar], [Publisher]

[8]. Claudel M., Schwarte J.V., Fromm K.M., New antimicrobial strategies based on metal complexes, *Chemistry*, 2020, **2**:849 [Crossref], [Google Scholar], [Publisher]

[9]. Das A., Das A., Banik B.K., Influence of dipole moments on the medicinal activities of diverse organic compounds, *Journal of the Indian Chemical Society*, 2021, **98**:100005 [Crossref], [Google Scholar], [Publisher]

[10]. Smith C.B., Days L.C., Alajroush D.R., Faye K., Khodour Y., Beebe S.J., Holder A.A., Photodynamic Therapy of Inorganic Complexes for the Treatment of Cancer, *Photochemistry and Photobiology*, 2022, **98**:17 [Crossref], [Google Scholar], [Publisher]

[11]. Karami A., Mohamed O., Ahmed A., Husseini G.A., Sabouni R., Recent advances in metal-organic frameworks as anticancer drug delivery systems: a review, Anti-Cancer Agents in Medicinal Chemistry (Formerly Current Medicinal Chemistry-Anti-Cancer Agents), 2021, **21**:2487 [Crossref], [Google Scholar], [Publisher]

[12]. Sodhi R.K., Paul S., Metal complexes in medicine an overview and update from drug design perspective, *Cancer Therapy & Oncology International Journal,* 2019, **14**:25 [Crossref], [Google Scholar], [Publisher]

[13]. Hadi A.G., Jawad K., Yousif E., El-Hiti G.A., Alotaibi M.H., Ahmed D.S., Synthesis of telmisartan organotin (IV) complexes and their use as carbon dioxide capture media, *Molecules*, 2019, **24**:1631 [Crossref], [Google Scholar], [Publisher]

[14]. Martínez VR, Aguirre MV, Todaro JS, Ferrer EG, Williams PA. Improvement of the anticancer activities of telmisartan by Zn (II) complexation and mechanisms of action, *Biological trace element research*, 2020, **197**:454 [Crossref], [Google Scholar], [Publisher]

[15]. Martínez V.R., Aguirre M.V., Todaro J.S., Lima A.M., Stergiopulos N., Ferrer E.G., Williams P.A., Zinc complexation improves angiotensin II receptor type 1 blockade and in vivo antihypertensive activity of telmisartan, *Future Medicinal Chemistry*, 2021, **13**:13 [Crossref], [Google Scholar], [Publisher]

[16]. Islas M.S., Martinez Medina J.J., Lopez Tevez L.L., Rojo T., Lezama L., Griera Merino M., Calleros L., Cortes M.A., Rodriguez Puyol M., Echeverría G.A., Piro O.E., Antitumoral, antihypertensive, antimicrobial, and antioxidant effects of an octanuclear copper (II)-telmisartan complex with an hydrophobic nanometer hole, *Inorganic*

Chemistry, 2014, **53**:5724 [Crossref], [Google Scholar], [Publisher]

[17]. Bano S., Mohd A., Khan A.A., Siddiqi K.S., Complexation and mechanism of fluorescence quenching of telmisartan with Y (III) and Nd (III), *Journal of Chemical & Engineering Data*, 2010, **55**:5759 [Crossref], [Google Scholar], [Publisher]

[18]. Abid N., Khan A.M., Shujait S., Chaudhary K., Ikram M., Imran M., Haider J., Khan M., Khan Q., Maqbool M., Synthesis of nanomaterials using various top-down and bottom-up approaches, influencing factors, advantages, and disadvantages: A review, *Advances in Colloid and Interface Science*, 2021, **29**:102597 [Crossref], [Google Scholar], [Publisher]

[19]. Kalyankar T., Wadher S.J., Anitha K., Sominath D., Improvement of aqueous solubility and In-vitro drug release rate of Telmisartan using hydrophilic base by various dispersion techniques, *International Journal of PharmTech Research*, 2016, **9** [Google Scholar], [Publisher]

[20]. Swati S., Formulation and Evaluation of Immediate Release Telmisartan Tablets using Hydrophilic Polymers. *Asian Journal of Pharmaceutics (AJP)*, 2017, **11** [Crossref], [Google Scholar], [Publisher]

[21]. Doofan I.S., Donald K., Nguumbur I.E., Gbaa A.I., Godwin I., Synthesis and spectrophotometric properties of sodium metal carboxylates, *Science*, 2021, **9**:113 [Crossref], [Google Scholar], [Publisher]

[22]. El-Sonbati A.Z., Mahmoud W.H., Mohamed G.G., Diab M.A., Morgan S.M., Abbas S.Y., Synthesis, characterization of Schiff base metal complexes and their biological investigation, *Applied Organometallic Chemistry*, 2019, **33**:e5048 [Crossref], [Google Scholar], [Publisher]

[23]. Thompson J.M., Infrared spectroscopy, Jenny Stanford Publishing; 2018 [Google Scholar], [Publisher]

[24]. Chohan M.S., Attimarad M., Venugopala K.N., Nair A.B., Sreeharsha N., Molina E.I., Kotnal R.B., Shafi S., David M., Shinu P., Altaysan A.I., Sensitivity Enhanced Ecofriendly UV Spectrophotometric Methods for Quality Control of Telmisartan and Benidipine Formulations: Comparison of Whiteness and Greenness with HPLC Methods, *International journal of environmental research and public health*, 2022, **19**:7260 [Crossref], [Google Scholar], [Publisher]

[25]. Hamza A., Al-Sibaai A.A., Alwael H., Saigl Z.M., Alosaimi E.H., Refat M.S., El-Shahawi M.S., Synthesis, ligation characteristics and analytical utility of the Schiff base (E)-1-[4-(2, 4-dihydroxybenzylidene)-amino) ethanone and its precious group metal (Ru^{3+}, Pt^{4+} & Ir^{3+}) complexes, *Results in Chemistry*, 2022, **4**:100422 [Crossref], [Google Scholar], [Publisher]

[26]. Alibrahim K.A., Al-Saif F.A., Bakhsh H.A., Refat M.S., Synthesis, physicochemical, and biological studies of new pyridoxine hcl mononuclear drug complexes of V (III), Ru (III), Pt (II), Se (IV), and Au (III) Metal Ions, *Russian Journal of General Chemistry*, 2018, **88**:2400 [Crossref], [Google Scholar], [Publisher]

[27]. Yan Y., Manickam S., Lester E., Wu T., Pang C.H., Synthesis of graphene oxide and graphene quantum dots from miscanthus via ultrasound-assisted mechano-chemical cracking method, *Ultrasonics Sonochemistry*, 2021, **73**:105519 [Crossref], [Google Scholar], [Publisher].

[28]. Abouzayed F.I., Emam S.M., Abouel-Enein S.A., Synthesis, characterization and biological activity of nano-sized Co (II), Ni (II), Cu (II), Pd (II) and Ru (III) complexes of tetradentate hydrazone ligand, *Journal of Molecular Structure*, 2020, **1216**:128314 [Crossref], [Google Scholar], [Publisher]

[29]. Kalimuthu K., Cha B.S., Kim S., Park K.S., Eco-friendly synthesis and biomedical applications of gold nanoparticles: A review, *Microchemical Journal*, 2020, **152**:104296 [Crossref], [Google Scholar], [Publisher]

[30]. Kunnumakkara A.B., Bordoloi D., Sailo B.L., Roy N.K., Thakur K.K., Banik K., Shakibaei M., Gupta S.C., Aggarwal B.B., Cancer drug development: The missing links, *Experimental Biology and Medicine*, 2019, **244**:663 [Crossref], [Google Scholar], [Publisher]

[31]. Kobara H., Fujihara S., Iwama H., Matsui T., Fujimori A., Chiyo T., Tingting S., Kobayashi N., Nishiyama N., Yachida T., Tadokoro T., Oura K., Tani J., Fujita K., Nomura T., Yoneyama H., Morishita A., Okano K., Suzuki Y., Mori H., Masaki T., Antihypertensive drug telmisartan inhibits cell proliferation of gastrointestinal stromal tumor

cells in vitro, *Molecular Medicine Reports*, 2020, **22**:1063 [Crossref], [Google Scholar], [Publisher].
[32]. Aljarba N.H., Imtiaz S., Anwar N., Alanazi I.S., Alkahtani S., Anticancer and microbial activities of gold nanoparticles: A mechanistic review, *Journal of King Saud University-Science*, 2022, **12**:101907 [Crossref], [Google Scholar], [Publisher]
[33]. Zeng L., Gupta P., Chen Y., Wang E., Ji L., Chao H., Chen Z.S., The development of anticancer ruthenium (II) complexes: from single molecule compounds to nanomaterials, *Chemical Society Reviews*, 2017, **46**:5771 [Crossref], [Google Scholar], [Publisher]

HOW TO CITE THIS ARTICLE
Zahraa Q. Mahdi, Mahasin F. Alias. Synthesis and Characterization of Bulky and Nano Complexes of Telmisartan with Some Heavy Metal Ions (Ru^{3+} and Au^{3+}) and Their Anticancer Activity. *J. Med. Chem. Sci*., 2023, 6(3) 677-692
https://doi.org/10.26655/JMCHEMSCI.2023.3.24
URL: http://www.jmchemsci.com/article_158432.html